Reconstruction of the CoGa(100) surface studied by thermal-energy helium-atom scattering, LEED, and AES

F. M. Pan,* Ch. Pflitsch, R. David, L. K. Verheij, and R. Franchy
Institut für Grenzflächenforschung und Vakuumphysik, Forschungszentrum Jülich, D-52425 Jülich, Germany
(Received 12 July 2000; published 13 March 2001)

The surface structure of CoGa(100) has been studied by means of thermal-energy helium-atom scattering (TEAS), low-energy electron diffraction (LEED), and Auger electron spectroscopy (AES). A $c(4\times2)$ surface reconstruction is revealed by LEED and TEAS measurements. Sometimes this reconstruction is mixed with a $(\sqrt{5}\times\sqrt{5})$ reconstruction, which is found to be due to a very minor contamination with oxygen. Only double-layer steps are found on the surface. Above 500 K, the reconstructed layer starts to disorder, but short-range ordering in this layer is still observed until 700 K. Near 900 K, segregation of Co is observed with AES. The increase of the cobalt concentration is consistent with filling up the 0.25 ML, necessary for the $c(4\times2)$ reconstruction, to a completed monolayer at 900 K. This interpretation implies that the surface is always terminated by Co.

DOI: 10.1103/PhysRevB.63.125414 PACS number(s): 61.18.Bn, 68.35.Bs

I. INTRODUCTION

Recently much interest has been devoted to the oxides of metal alloy surfaces because of their intrinsic significance[1] and possible application potentials ranging from microelectronics and heterogeneous catalysis to material science.[2] Stimulated by both basic and applied potentials, extensive investigations of Ga oxides on the CoGa surface have been performed by means of low-energy electron diffraction (LEED), Auger-electron spectroscopy (AES), scanning tunneling microscopy (STM), and electron energy-loss spectroscopy.[3–5] CoGa is an intermetallic alloy ordering in a CsCl-type structure with a lattice constant of 2.88 Å. The (100) layers have an *ABAB* . . . stacking sequence and consequently, it is expected that the surface is terminated by either Co or Ga for the bulk termination. Because the surface properties play an important role in the oxidation of the surface, knowing the intrinsic properties of the clean CoGa surfaces is necessary in order to understand and control the oxidation process.

Thermal-energy He-atom scattering (TEAS) has been demonstrated to be a valuable tool for investigating surface structures and their ordering and disordering dynamics.[6–11] In this work we have studied the surface structure and morphology of clean CoGa(100) with help of TEAS in combination with LEED and AES. It has been well established that the atomic surface structure of alloy and compound crystals may differ from that in the bulk. For instance, the surface reconstructs in order to stabilize the surface by reducing the surface energy.[12] The CoGa(100) surface shows a $c(4\times2)$ reconstruction. Sometimes, one observes in addition $(\sqrt{5}\times\sqrt{5})$ reconstruction.[13] In this work this reconstruction is found to be induced by a very low contamination of oxygen below the detection limit of our AES system. The $c(4\times2)$ reconstruction, characteristic for the clean CoGa(100) surface, is found to disorder between 500 and 700 K. Above 800 K a compositional change of the surface is observed that indicates that the CoGa(100) crystal is terminated with a Co layer.

II. EXPERIMENT

The experiments have been performed in an ultrahigh vacuum (UHV) helium-scattering apparatus at a base pressure of 5×10^{-11} mbar. The UHV apparatus is equipped with a supersonic helium nozzle beam with a quadrupole mass spectrometer as detector, LEED optics, AES, and a mass spectrometer for residual gas analysis. The apparatus is described in detail in a previous paper.[14] The energy of the He-beam E_{He} can be varied between 14 and 100 meV by cooling or heating the nozzle. The incident He beam and the detector are fixed in a rectangular geometry, i.e., the total scattering angle is $\theta_i+\theta_f=90°$, where θ_i and θ_f are the angles of the incident and scattered beams, respectively, with respect to the surface normal. In angular scans the polar angle of the sample is varied and consequently θ_i and θ_f change together. In the scans, the scattered intensity is shown as a function of the momentum transfer parallel to the surface, $q_{\parallel}=k_i(\sin\theta_i-\sin\theta_f)$ where k_i is the wave vector of the He beam. Interference curves are obtained by measuring the specular intensity as a function of k_i, where k_i is varied by changing the energy of the He beam (temperature of the nozzle). In this study, all diffraction spectra (angular scans) were measured with $k_i=7.1\,\text{Å}^{-1}$ $(E_{\mathrm{He}}=26\,\mathrm{meV},\lambda_i=0.89\,\text{Å})$. The energy resolution $(\Delta E/E)$ at this energy is 1.2% according to time-of-flight diffraction measurements.

The CoGa(100) single crystal was cut by spark erosion and polished mechanically. It was oriented with an accuracy better than 0.5°. AES measurements showed that the main impurities were oxygen, carbon, and sulfur. Heating the sample in an oxygen atmosphere ($P_{\mathrm{O_2}}\approx1\times10^{-6}$ mbar) at 800 K leads to the oxidation of the carbon and sulfur impurities. Further annealing at 1070 K for 8 min leads to the desorption of the oxides and produces a clean CoGa(100) surface.

III. RESULTS AND DISCUSSION

A. Surface structural characterization by LEED and TEAS

Figure 1 shows the LEED pattern for the clean CoGa(100) surface at room temperature. Besides the main

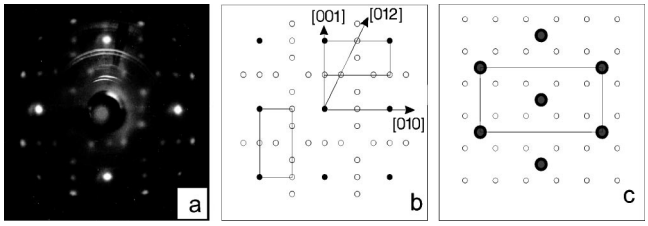

FIG. 1. (a) LEED pattern of the CoGa(100) surface, $E = 88$ eV. (b) Schematic presentation of the LEED pattern. The two rectangles show two $c(4\times2)$ domains, oriented normal to each other. The solid circles represent the (0,0), (±1,0), (0,±1), and ($\pm1,\pm1$) diffraction spots, while the open circles correspond to the extra diffractions of the $c(4\times2)$ reconstruction (c) Real-space model of one domain of the $c(4\times2)$ reconstruction. The solid circles represent adatoms of one kind (Co, see Sec. III D), the open circles represent the underlying layer consisting of the other kind of atoms (Ga).

diffraction spots of an unreconstructed (1×1) surface, extra diffraction spots are found, which corresponds to a $c(4\times2)$ reconstruction, with two domains that are normal to each other. A real space model of one of the domains of the reconstruction is shown in Fig. 1(c). The reconstruction is schematically illustrated in Fig. 1(b) in the reciprocal space, where the solid circles represent the main diffraction spots [(0,0),(±1,0),(0,±1),($\pm1,\pm1$)], and the open ones result from the two domains of the reconstructed structure, e.g., in the [001] direction the $(0,\frac{1}{2})$ and in the [012] direction the $(\frac{1}{4},\frac{1}{2})$ and the $(\frac{1}{2},1)$ spots.

The structure of the CoGa(100) surface is also studied by TEAS. We have performed angular He-scattering scans at different azimuths from 0° to 45° in steps of 0.5°. Considering the symmetry of the surface this procedure explores the surface morphology in all azimuthal directions. The results show the same diffraction distributions as LEED does. Figure 2 shows the diffraction spectra of TEAS from the CoGa(100) surface along two principal reciprocal directions [001] and [012]. The diffraction distributions are consistent with the $c(4\times2)$ structure.

Since we use a fixed rectangular scattering geometry ($\theta_i + \theta_f = 90°$) in our experiment, the momentum transfer $q_\parallel$ corresponding to the diffraction peaks is related to θ_i and the periodicity a of the surface as

$$q_\parallel = k_i(\sin\theta_f - \sin\theta_i) = k_i(\cos\theta_i - \sin\theta_i) = \frac{n2\pi}{a}, \quad (1)$$

where $n = 0,1,2,\ldots$ and k_i is the wave vector of the incident helium beam. The positions of the diffraction peaks in Figs. 2(a) and 2(b) agree within 0.3% with the expected positions for the $c(4\times2)$ reconstructed structure of the CoGa(100) surface.

The curve at the bottom in Fig. 2(b) is measured on CoGa(100) after oxidizing the surface and subsequent annealing at 1070 K. After annealing, no oxygen is detected with AES. In comparison with the other diffraction curves, additional peaks are seen (indicated by arrows). These diffraction peaks correspond to a $(\sqrt{5}\times\sqrt{5})$ structure. It is

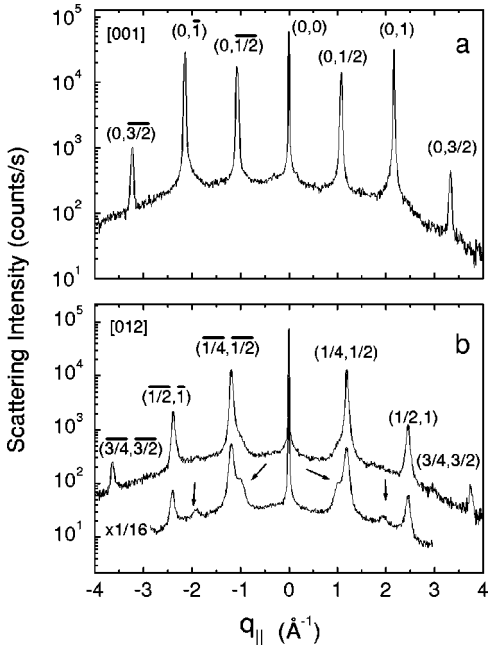

FIG. 2. He-diffraction spectra of the CoGa(100) surface along the: (a) [001] and (b) [012] direction. The arrows in (b) indicate the $(\sqrt{5}\times\sqrt{5})$ reconstruction.

found that the additional peaks in the helium diffraction spectra [arrows indicated in Fig. 2(b)] disappear after several cycles of sputtering and annealing, indicating that the $(\sqrt{5}\times\sqrt{5})$ structure is related to an oxygen contamination of the crystal surface. However, oxygen could not be detected by AES on the surface, so the $(\sqrt{5}\times\sqrt{5})$ diffraction peaks are induced by a very low oxygen concentration. The $(\sqrt{5}\times\sqrt{5})$ structure has been found previously by LEED and STM.[13] Figure 3 shows a STM image of the clean CoGa(100) surface with a scan width of 320×320 Å^2. In this figure domains with the $c(4\times2)$ reconstruction are represented by rectangles and the $(\sqrt{5}\times\sqrt{5})$ reconstruction by the square. The white dots that form the reconstructions are interpreted as adatoms,[4] as illustrated for the $c(4\times2)$ structure in Fig. 1(c). The corrugation in the reconstructions in as far as it can be resolved by STM is 0.3 Å. The black dots in the STM image are interpreted as oxygen atoms adsorbed on the surface.[4]

The quality of the surface can be characterized in terms of the width of the diffraction peaks.[15–18] For instance, the step density (mean terrace width) can be estimated from the full width at half maximum Δq of the specular peak. According to the specular peak profile in Fig. 2, $\Delta q = 0.021$ Å^{-1}, which corresponds to a terrace width ($\overline{\Delta} = 2\pi/\Delta q$) of about 300 Å. Taking into account the transfer width of the apparatus[19] and crystal imperfections, we can conclude that the mean terrace width is at least 300 Å.

B. Surface steps and terrace height

Interference curves (see Sec. II) contain information on step height and layer distribution.[10] When changing the vertical component of the incident He wave vector (by varying

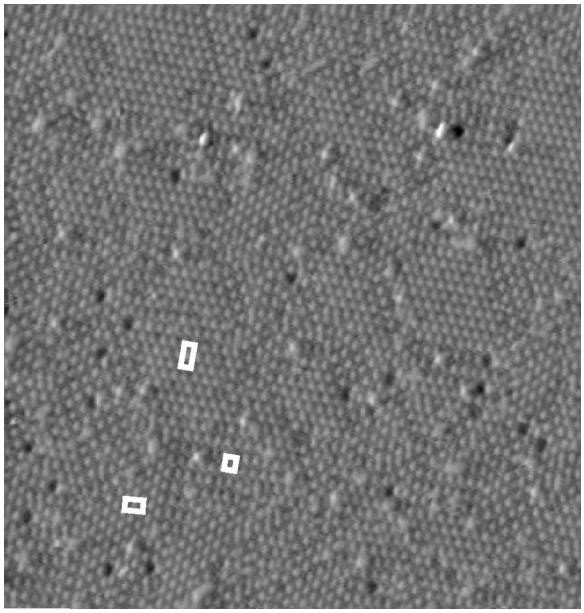

FIG. 3. STM image of the CoGa(100) surface at atomic resolution showing the $c(4\times2)$ (rectangles) and the $(\sqrt{5}\times\sqrt{5})$ (square) reconstructions. Reproduced from the Ph.D. thesis of G. Schmitz (Fig. 4.7) (Ref. 13).

the incident angle or the energy of the He beam), the diffraction intensities will oscillate due to the alternating in-phase (constructive) and anti-phase (destructive) interference of the atom wave scattering from neighboring terraces. Maxima and minima of the specular intensity are observed when the phase shift meets the condition

$$\varphi = 2dk_i \cos\theta_i = dq_\perp = n2\pi, \tag{2}$$

where d is the step height, n is integer for in-phase and half-integer for anti-phase interference and $q_\perp$ is the wave vector transfer perpendicular to the surface.

Figure 4 shows the interference curve measured on the clean CoGa(100) surface. The wave vector normal to the surface $q_\perp$ is varied by changing the energy of the incident He beam. In principle, the step height can be easily derived from the distance between two neighboring interference peaks. Information on the layer distribution can be obtained from an analysis of the shape of the interference curve. In practice the situation appears to be more complicated, as is already clear from the observation that the distance between the first and the second maximum in Fig. 4 is not the same as the distance between the second and the third maximum. The reason seems to be that multiple scattering effects, such as selective adsorption,[20] cannot be neglected. Indeed, several fine dips and peaks, superimposed on the main peaks, are observed, which suggest that selective adsorption takes place. Therefore, we have analyzed the curve in Fig. 4 in more detail only at the higher beam energies, where the influence of such effects should be less.

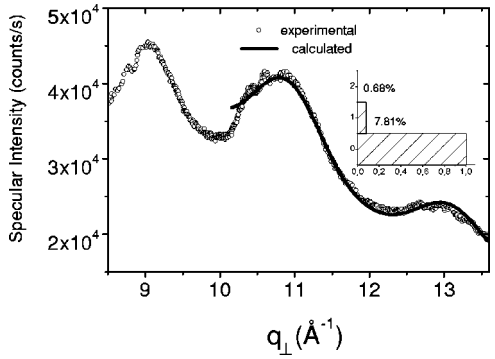

FIG. 4. The specular intensity as a function of vertical momentum transfer $q_\perp$ of the He beam. The measurement is performed along the [001] azimuth. The experimental data (open circles) are fitted for values between 10.2 and 13.6 $Å^{-1}$ (solid line) assuming that three surface layers are visible to the helium beam (within a distance equal to the transfer width of the apparatus). The inset shows the coverage of the three layers as obtained from the fit.

For the analysis, we used a simple model that assumes coherent overlap of plane waves emerging from different terrace levels. The scattered specular intensity is then given by[10]

$$I(q_i) = I_0 e^{-\alpha E_i}\left|\sum_{j=0}^{\infty} a_j e^{-ij\varphi(q_i)}\right|^2. \tag{3}$$

Here I_0 is the specular intensity from an ideal surface without steps. The first exponentials decay term attributes to the Debye-Waller effect,[21] a_j is the visible fraction of jth level terrace and $\varphi(q_\perp)$ the phase shift as defined in Eq. (2). The solid line in Fig. 4 represents the best fit of the experimental results using Eq. (3).

The surface step height is determined to be 2.85 Å which agrees quite well with double layer steps on the clean CoGa(100) surface. This result is also supported by STM investigations as shown in Fig. 5.[22] The STM image taken at 300 K with a scan width of 360×360 $Å^2$ shows an area of the CoGa(100) surface with a high step density. Two neighboring terraces are always separated by double atomic steps. The fact that the terraces are separated by double atomic steps strongly suggests that only one of the two possible surface terminations, i.e., a Co or a Ga layer, is stable. Using this step height, the first maximum in Fig. 4 should be found at 8.8 $Å^{-1}$, i.e., at the position of the small shoulder seen in the curve and about 0.2 $Å^{-1}$ below the main maximum.

The layer distribution obtained from fitting Eq. (3) is shown in Fig. 4 as inset. Within the transfer width (about 400 Å) of our helium-scattering equipment, three terrace levels are present. The coverage of these layers is shown in the inset. The visible fraction of the layers is $a_0 = 100\% - 7.81\% \approx 92\%$, $a_1 \approx 7\%$, and $a_2 \approx 0.7\%$. Though, one should consider this result with care because of the simplicity of the model, it does indicate that the clean CoGa(100) surface is quite flat.

C. Temperature dependence of the surface structure

In order to study the temperature dependence on CoGa(100) surface structure, angular scans have been measured for surface temperatures from room temperature up to 900 K along the principal [001] and [012] azimuths, as

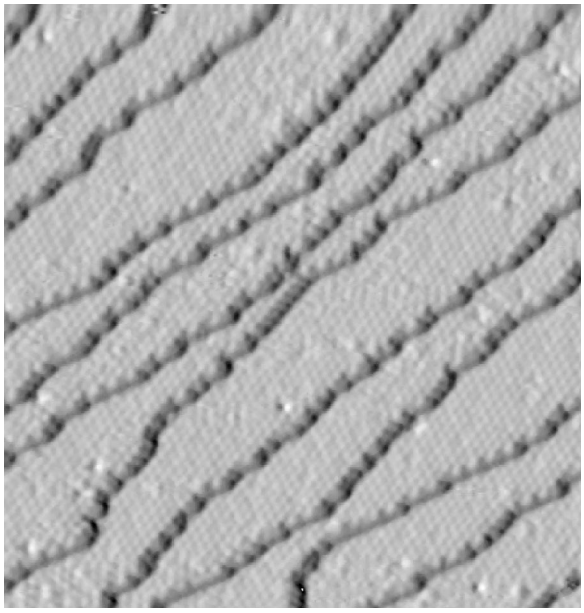

FIG. 5. STM image of the CoGa(100) surface showing steps with a height of ~2.9 Å. The scan area is 360×360 Å^2, $I=0.9$ nA, $U=1.26$ V. Reproduced from the Ph.D. thesis of P. Gassmann (Fig. 7.4) (Ref. 22).

shown in Figs. 6 and 7, respectively. At low temperature the surface is stable as observed from LEED and TEAS. Between 400 and 500 K, the peaks (indicated by arrows in Fig. 7) related to the $(\sqrt{5}\times\sqrt{5})$ reconstruction disappear. The $c(4\times2)$ reconstruction is still stable in this temperature range. The half-order peaks $(0,\pm\frac{1}{2})$ (Fig. 6) and $(1,\pm\frac{1}{2})$ (Fig. 7) decrease somewhat faster than the specular peak does, but they remain clearly visible. Upon heating the sample to 600 K, the half-order peaks disappear, whereas the $(\pm\frac{1}{4},\pm\frac{1}{2})$ (Fig. 7), the $(0,\pm1)$ (Fig. 6), and the specular peaks are conserved. We interpret this as a loss of long-range order of the $c(4\times2)$ reconstruction. On a short range, however, the order of this structure is conserved, as shown by the broad $(\pm\frac{1}{4},\pm\frac{1}{2})$ peaks (Fig. 7) that remain clearly visible up to 700 K.

Between 800 and 900 K the first-order diffraction peaks disappear, whereas the specular peak remains clearly present even at this high temperature. In order to elucidate the high-temperature behavior in more detail, we have measured the

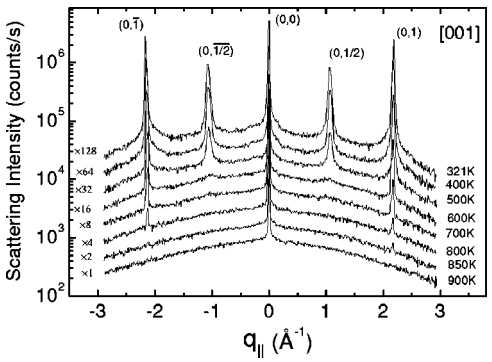

FIG. 6. He-diffraction spectra, measured along the [001] azimuth of the CoGa(100) surface at different surface temperatures.

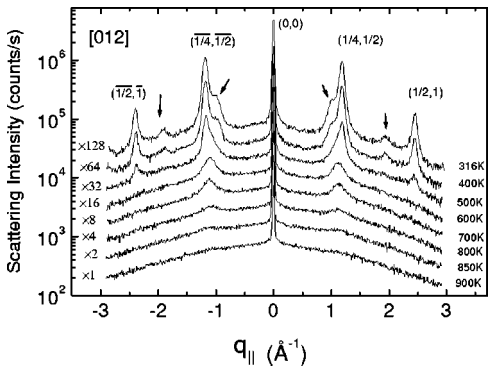

FIG. 7. He-diffraction spectra, measured along the [012] azimuth of the CoGa(100) surface at different surface temperatures. The arrows indicate diffraction peaks form a coexistent $(\sqrt{5}\times\sqrt{5})$ surface reconstruction, which originates from a very low oxygen contamination.

temperature dependence of the specular peak $I(T)$ quantitatively. From the dependence measured below 400 K, an effective Debye-Waller (DW) factor, i.e., the DW factor as seen with He scattering, can be determined, which is used to correct the specular intensities measured at higher temperatures.

The DW factor is defined as $e^{-2W(T)}=I(T)/I_0$, and a simple expression of $W(T)$ is given by[23,24]

$$W(T)=\frac{12m(E_i\cos^2\theta_i+D)T}{Mk_B\Theta_D^2}. \tag{4}$$

Here m is the incident particle mass, D the well depth (Beeby correction[25]), which is typically 5–8 meV.[26] M is the mass of a surface atom, k_B the Boltzmann constant, and Θ_D the surface Debye temperature. Figure 8 presents the specular He intensity as a function of the surface temperature between 100 and 500 K. From the best-fit of this curve, we get $2W(T)=(3.7\pm0.1)\times10^{-3}$ T. The surface Debye temperature for CoGa(100) corresponding to this DW factor is (214 ± 6) K in the case of Co termination of the surface or (197 ± 5) K in the case of Ga termination.

Corrected for the Debye-Waller effect, the intensity of the specular peak vs surface temperature in the range 300–900 K is shown in Fig. 9. It is interesting to note that the specular

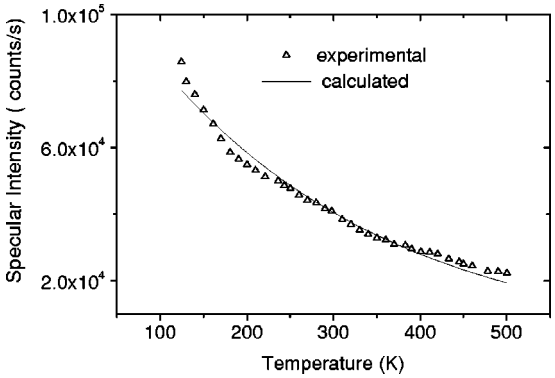

FIG. 8. Specular intensity as a function of sample temperature. The solid line is the best-fit of the experimental results (triangle).

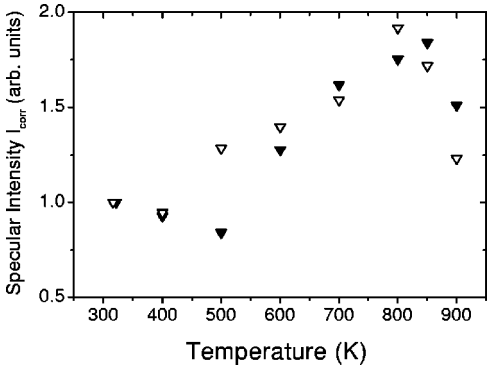

FIG. 9. Debye-Waller corrected specular intensity I_{corr} vs sample temperature for the CoGa(100) surface. Two data sets are shown, measured in the [001] (τ) and the [012] (∇) direction.

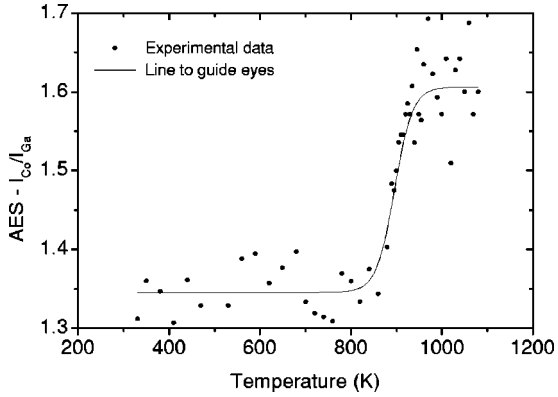

FIG. 10. AES peak-to-peak intensity ratio of Co (775 eV) and Ga (1070 eV) as a function of sample temperature.

intensity corrected for the DW attenuation I_{corr} increases with increasing sample temperature, whereas all the nonspecular peaks, even after correction for the DW effect, decrease with increasing temperature. Although the increase of I_{corr} seems to indicate that some kind of ordering is taking place, it can also be explained in terms of disordering of the reconstructed surface, i.e., in agreement with the explanation given for the disappearance of the other diffraction peaks. With respect to specular scattering, one can consider the CoGa(100) surface as a flat and hardly corrugated first layer with an ordered (below 500 K) or disordered (above 500 K) overlayer of 0.25 ML. If the overlayer is ordered or if the area around an atom with disordered surrounding, which scatters the He atoms diffusely, is smaller than the area of the unit cell in the reconstructed overlayer, then there is no overlap of such ''diffuse scattering areas.'' In that case one can argue that the so-defined ''diffuse scattering area'' does not contribute to the specular diffraction peak, i.e., it contributes either to the diffuse background or to the nonspecular diffraction peaks. When the overlayer is ordered, these areas do not overlap, so the sum of these areas is the maximum which is possible. Upon disordering of the overlayer, some of the diffuse scattering areas will start to overlap, so that the area (of the first layer), which contributes to specular scattering, increases. Thus one expects the specular intensity to increase upon disordering in this specific case.

At around 800 K, I_{corr} has a maximum and starts to decrease above this temperature. However, in that temperature region also a change in the surface composition is found, as discussed in the next section.

D. Co segregation to the surface at high temperature

Information on the surface composition of the CoGa(100) crystal can be obtained by measuring the intensities of the Co (775 eV) and Ga (1070 eV) Auger transitions. Figure 10 shows the peak-to-peak intensity ratio of the Co (775 eV) and Ga (1070 eV) transitions. In the temperature range 300–800 K the ratio is constant. An obvious enhancement of the AES signal I_{Co}/I_{Ga} is observed between 850 and 900 K. Above this temperature, the ratio stabilizes again at a new level. The experimental results are reversible with respect to temperature. Consequently, we conclude that the relative amount of surface Co increases between 850 and 900 K.

The Co enrichment can be explained in terms of a simple model. CoGa is an intermetallic alloy ordering in a CsCl-type structure and the (100) layers have an *ABAB* . . . stacking sequence. The reconstructed $c(4\times2)$ topmost layer is assumed to consist of 0.25 ML of either Co or Ga. Heating the surface above 900 K results in a surface with a different but again well-defined composition. Since the surface does not show any evidence for a superstructure, it seems very likely that this new phase consists of $a(1\times1)$ structure. As the surface is enriched with Co above 900 K, the surface layer can only consist of Co. Thus, according to this simple model, we only have to consider the phase transitions from a surface terminated with either 0.25 ML of Ga or Co to a surface terminated with a complete Co layer.

The AES intensities I_{Co} and I_{Ga} from the reconstructed surface can be calculated in first approximation by

$$I_{Co}=I^0_{Co}F(E_{Co})[a+(1-a)\exp(-d_{Ga}/\lambda_{Co})]$$

and

$$I_{Ga}=I^0_{Ga}F(E_{Ga})[1-a+a\exp(-d_{Co}/\lambda_{Ga})]. \qquad (5)$$

Here I^0 is the AES signal from the pure bulk, $F(E_{CoGa})$ is a function of the Co (Ga) Auger electron energy, a is the relative amount of Co (in terms of ML) in the overlayer or in the first layer not covered by Ga, d is the thickness of a Co or Ga overlayer, and λ the inelastic mean free path of electrons. For a Co terminated $c(4\times2)$ structure (with 0.25 ML Co overlayer) $a=0.25$, and for a Ga terminated $c(4\times2)$ structure (the first Co layer is covered by 0.25 ML Ga) $a=0.75$. After the phase transition to the Co(1×1) surface, the respective AES intensities of Co and Ga are

$$I'_{Co}=I^0_{Co}F(E_{Co})$$

and

$$I'_{Ga}=I^0_{Ga}F(E_{Ga})\exp(-d_{Co}/\lambda_{Ga}). \qquad (6)$$

The ratio of I_{Co}/I_{Ga} measured after and before the enrichment is then equal to

$$\frac{I'_{Co}/I'_{Ga}}{I_{Co}/I_{Ga}} = \frac{a+(1-a)\exp(d_{Co}/\lambda_{Ga})}{a+(1-a)\exp(-d_{Ga}/\lambda_{Co})}. \quad (7)$$

Taking the same thickness for the Co and Ga layers, $1.44/\cos(\beta)$ Å, where $\beta = 42°$ is the detection angle of the AES system, and assuming $\lambda_{Ga} = (E_{Ga}/E_{Co})^{1/2}\lambda_{Co}$, we get $\lambda_{Co} = 14.7 \pm 3$ Å in the case of Co termination ($a = 0.25$) and $\lambda_{Co} = 5.0 \pm 1.5$ Å in the case of Ga termination ($a = 0.75$) if a change of 1.2 ± 0.05 (Fig. 10) is inserted in Eq. (7). According to Seah and Dench,[27] the mean free path λ_{Co} for 775 eV electrons is 12.5 Å with an estimated accuracy of around 30%. Consequently, we conclude that our AES results essentially exclude the possibility that the $c(4\times2)$ CoGa(100) surface is Ga terminated.

Another model for the crystal structure at room temperature that could explain the Co enrichment observed with AES would be a crystal terminated by a Ga layer of which 0.25 ML is replaced by Co. The mean free path λ_{Co} corresponding to the observed increase of the AES signal would be 10.5 ± 2 Å if it is assumed that this surface reconstructs to a Co terminated surface at 900 K. It is clear that our AES measurement cannot exclude this possibility. However, such a structure with 0.75 ML Ga and 0.25 ML Co in the outermost surface layer seems to be only compatible with the STM and the He-scattering experiments if a relatively large outward relaxation of the Co atoms is assumed. Without a relaxation of at least several tenths of an angstrom, one would not expect to observe, on a metallic surface, a corrugation of 0.3 Å between atoms, which are very close to each other in the Periodic Table and are only 2.88 Å apart in the surface (Figs. 3 and 5). Also the large first-order diffraction peak, which is about half the height of the specular peak, indicates that the corrugation is much larger than could be expected for a metallic surface with interatomic distances of 2.88 Å. For instance, on a copper surface the intensity of the first-order peak in the (100) direction (interatomic distance $= 3.6$ Å) is only 5% of the specular intensity.[28]

Our result suggests that the CoGa(100) surface is always terminated by Co, probably as a 0.25 ML on top of a Ga layer, but possibly as a 0.25 ML sticking out of a Ga layer. Though one needs total energy calculations to show what the reason is for the stability of this reconstruction, one may speculate that it is related to the lower free energy of a hcp Co(0001) surface [or a fcc Co(111) surface] relative to both a Ga terminated surface and to a bcc Co(100) surface. According to this idea, bonding of the Ga surface atoms to one Co atom on top would be sufficient to reduce the surface energy below the surface energy of a bcc Co(100) surface. Since the $c(4\times2)$ reconstruction of the CoGa surface may also be seen as a distorted $(\sqrt{7},\sqrt{7})$ reconstruction relative to a hcp Co(0001) surface, one could see the $c(4\times2)$ reconstruction as the beginning of the formation of a stable Co surface. For reconstructions with a larger density, the misfit between the Co(0001) surface and the CoGa surface would become too large to result in a further lowering of the surface energy.

IV. CONCLUSIONS

The structure of the CoGa(100) surface was investigated by means of TEAS, LEED, and AES. At room temperature a $c(4\times2)$ surface reconstruction of the CoGa surface is found which is sometimes accompanied by a $(\sqrt{5}\times\sqrt{5})$ reconstruction. The $c(4\times2)$ reconstruction is found to be characteristic for the clean surface. The $(\sqrt{5}\times\sqrt{5})$ structure is probably due to an oxygen contamination with a concentration below the detection limit of our AES system.

Interference measurements show the evidence for double-layer steps, which indicates that the surface is always terminated by the same atomic species. In the temperature range between 500 and 700 K an order-disorder phase transition of the reconstructed $c(4\times2)$ layer is observed. At 700 K some short-range order still remains. Between 850 and 900 K a second phase transition is found, in which the composition of the surface changes: About 0.75 ML of Co segregates onto the surface. At this temperature, the surface matches a transition from a very disordered $c(4\times2)$ reconstruction to a (1×1) surface that seems to be composed only of Co. This conclusion implies that the CoGa(100) surface is also Co terminated at the lower temperatures.

ACKNOWLEDGMENT

This work was supported by the HGF project—Magnetoelectronics.

*Corresponding author. Email address: f.m.pan@fz-juelich.de

[1] A. Atkinson, Rev. Mod. Phys. **57**, 437 (1985).
[2] R. Franchy, Surf. Sci. Rep. **38**, 195 (2000).
[3] R. Franchy, G. Schmitz, P. Gassmann, and F. Bartolucci, Appl. Phys. A: Mater. Sci. Process. **65**, 551 (1997).
[4] G. Schmitz, P. Gassmann, and R. Franchy, Surf. Sci. **397**, 339 (1998).
[5] M. Eumann, G. Schmitz, and R. Franchy, Appl. Phys. Lett. **72**, 3440 (1998).
[6] Bene Poelsema and George Comsa, in *Scattering of Thermal Energy Atoms*, STMP Vol. 115 (Springer-Verlag, Berlin, 1989).
[7] C. Tölkes, R. Struck, R. David, P. Zeppenfeld, and G. Comsa, Phys. Rev. Lett. **80**, 2877 (1998).
[8] J. Ellis, A. P. Graham, and J. P. Toennies, Phys. Rev. Lett. **82**, 5072 (1999).
[9] A. T. Pasteur, X.-C. Guo, T. Ali, M. Gruyters, and D. A. King, Surf. Sci. **366**, 564 (1996).
[10] C. Tölkes, P. Zeppenfeld, M. A. Krzyzowski, R. David, and G. Comsa, Phys. Rev. B **55**, 13 932 (1997).
[11] D. Farías and K. H. Rieder, Rep. Prog. Phys. **61**, 1575 (1998).
[12] D. Grozea, E. Landree, C. C. Davila, E. Benga, R. Plass, and L. D. Marks, Micron **30**, 41 (1999).
[13] G. Schmitz, Ph.D. thesis, Universität Düsseldorf, Berichte des Forschungszentrums Jülich 3634, 1999.
[14] K. E. Kuhnke, K. Kern, R. David, and G. Comsa, Rev. Sci. Instrum. **65**, 3458 (1994).
[15] L. Verheij, J. Lux, and B. Poelsema, Surf. Sci. **144**, 385 (1984).
[16] M. Henzler, Appl. Surf. Sci. **11/12**, 450 (1982).
[17] C. S. Lent and P. I. Cohen, Surf. Sci. **139**, 121 (1984).
[18] J. Wollschläger, J. Falta, and M. Henzler, Appl. Phys. A: Solids

Surf. **50**, 57 (1990).
[19] G. Comsa, Surf. Sci. **81**, 57 (1979).
[20] H. Hoinkes and H. Wilsch, in *Helium Atom Scattering from Surfaces*, edited by E. Hulpke (Springer-Verlag, Berlin, 1992), p. 13.
[21] V. Bortolani *et al.*, Surf. Sci. **208**, 1 (1989).
[22] P. Gassmann, Ph.D. thesis, RWTH-Aachen, Berichte des Forschungszentrums Jülich-3305, 1996.
[23] A. C. Levi and H. Suhl, Surf. Sci. **88**, 221 (1979).
[24] J. H. Weare, J. Chem. Phys. **61**, 2900 (1974).
[25] J. L. Beeby, J. Phys. C **4**, L359 (1971).
[26] J. P. Toennies, in *Surface Phonons*, edited by W. Kress and F. W. de Wette, Springer Series in Surface Science Vol. 21 (Springer, Berlin, 1991), p. 111.
[27] M. P. Seah and W. A. Dench, Surf. Interface Anal. **1**, 2 (1979).
[28] Ch. Pflitsch, R. David, L. Verheij, and R. Franchy, Surf. Sci. (unpublished).